

Comment on “Multiscatter stellar capture of dark matter”

Cosmin Ilie,* Jacob Pilawa, and Saiyang Zhang
Department of Physics and Astronomy, Colgate University
13 Oak Dr., Hamilton, NY 13346, U.S.A.
(Dated: April 4, 2022)

Bramante, Delgado, and Martin [Phys. Rev. D **96**, 063002(2017)., hereafter BDM17] extended the analytical formalism of dark matter (DM) capture in a very important way, which allows, in principle, the use of compact astrophysical objects, such as neutron stars (NS), as dark matter detectors. In this comment, we point out the existence of a region in the dark matter neutron scattering cross section (σ_{nX}) vs. dark matter mass (m_X) where the constraining power of this method is lost. This corresponds to a maximal temperature (T_{crit}) the NS has to have, in order to serve as a dark matter detector. In addition, we point out several typos and errors in BDM17 that do not affect drastically their conclusions. Moreover, we provide semi-analytical approximations for the total capture rates of dark matter particle of arbitrary mass for various limiting regimes. Those analytical approximations are used to validate our numerical results.

Keywords: dark matter; dark matter capture; neutron stars; white dwarfs

* E-mail at: cilie@colgate.edu; Permanent Institution: Department of Theoretical Physics, National Institute for Physics and Nuclear Engineering, Magurele, P.O.Box M.G. 6, Romania

I. INTRODUCTION

The dark matter capture formalism was originally developed in the 1980s for the case of weakly interacting massive particles (WIMPS), which was the most common and well motivated dark matter (DM) candidate at the time. In [1], Press and Spergel estimate the capture rates of WIMPS by the Sun, whereas Gould generalizes this to more arbitrary massive astrophysical objects, including the Earth in [2]. Both of those seminal papers, which were used as the basis of most subsequent work on dark matter capture by astrophysical objects (e.g. [3–7]), are limited to the capture of dark matter by optically “thin” media; i.e. the DM particle will have, on average, at most one collision with a nucleus while it traverses the star. In the early 2000’s, an important step forward in this field was the paper by Albuquerque et al. [8], which deals with the opposite regime: the dark matter particle would need to collide an extremely large number of times in order to get captured. For a class of strongly interacting superheavy dark matter particles known as SIMPZILLAs, [8] finds analytic expressions for the capture rates by the Sun and the Earth. The intermediary regime, when a DM particle would have to collide with nuclei inside a star an order unity number of times remained out of reach until BDM17 [9] was published in 2017. The authors managed to calculate closed form, analytic expressions for the capture rates of dark matter of arbitrary mass with arbitrary cross scattering section by arbitrary astrophysical objects, thus opening up numerous avenues of research. The formalism in BDM17 is quite general and it has only on one simplifying assumption: that of replacing a kinematic geometric quantity with its average value, $\langle z \rangle$. Dasgupta, Gupta, and Ray managed to lift this restriction in [10]. Therefore, the theory of dark matter capture is now an almost complete chapter.

Below, we briefly summarize the multiscattering capture formalism of BDM17. The total capture rate can be written as a series, summing all partial capture rates C_N when the DM particle has been slowed down below the escape velocity by exactly N collisions:

$$C_{tot} = \sum_{N=1}^{\infty} C_N. \quad (1)$$

BDM17 provide analytical formulae for C_N . First, a simplifying assumption is made on the amount of energy lost by the dark matter particle in each scattering event: $\Delta E = z\beta_+ E_0$. This assumption amounts to replacing the general kinematic quantity z with its average value over all collisions: $\langle z \rangle$. In most generic situations $\langle z \rangle \approx 1/2$. Here $\beta_+ \equiv 4m_X m / (m_X + m)$, with m_X the DM mass and m the mass of the target nucleus. Following BDM17 we integrate over all possible incidence angles and DM velocities using a Maxwell-Boltzmann distribution with a DM dispersion velocity \bar{v} . We find, for capture of DM by an object where the local DM density is n_X :

$$C_N = \frac{1}{3} \pi R^2 p_N(\tau) \frac{\sqrt{6} n_X}{\sqrt{\pi} \bar{v}} \left((2\bar{v}^2 + 3v_{esc}^2) - (2\bar{v}^2 + 3v_N^2) \exp \left(-\frac{3(v_N^2 - v_{esc}^2)}{2\bar{v}^2} \right) \right), \quad (2)$$

where $v_N = v_{esc}(1 - \langle z \rangle \beta_+)^{-N/2}$ and $p_N(\tau)$ being the probability to collide exactly with N nuclei per crossing. The main parameter that controls this probability, and thus the capture rate, is the optical depth $\tau = 2R_* \sigma n_T$, where R_* is the radius of the star, σ is the cross section of the DM nucleus scattering, and n_T is the average number density of nuclei inside the star. We point out that we obtained an additional overall factor of $1/3$, when comparing our result with the one presented in Eq. 22 of BDM17.

Two of the authors of this comment have used the formalism of BDM17 to show that dark matter capture can impose an upper limit on the masses of the first stars in [11], hereafter known as IZ19. While working to explore the observable implications of IZ19 (see [12]), the authors of this comment identified another typo and several errors in BDM17. First, for the equation that gives the approximate capture rate after exactly N scatters in the limit when $m_X \gg m$ and $v_{esc} \gg \bar{v}$ (Eq. 23 of BDM17), we find, by taking the limit of Eq. 2, that the relative sign of the parenthetical term $\frac{2A_N^2 \bar{v}^2}{3v_{esc}^2}$ is actually $+$, not $-$ as in BDM17. Namely, Eq 23 of BDM17 should read:

$$C_N = \sqrt{24\pi} p_N(\tau) n_X G M_* R_* \frac{1}{\bar{v}} \left(1 - \left(1 + \frac{2A_N^2 \bar{v}^2}{3v_{esc}^2} \right) e^{-A_N^2} \right) \quad (3)$$

We also point out that the overall numerical factors between Eq. 22 and Eq. 23 of BDM17 are off by $1/3$. This further reinforces the point we made above, that Eq. 22 of BDM17 should be corrected by the inclusion of a factor of $1/3$, as in our Eq. 2.

Our main concern was first with the effects of the flip of sign pointed out in the discussion above Eq. 3 on our results of IZ19. We found in [13] that, for the parameter space explored in that paper, the term in question is subdominant and thus has no effects. After pointing out in a series of emails to the authors of BDM17 our concerns specified above,

with Eq. 22 and Eq. 23 of BDM17, we also decided to explore further any implications those might have on the results of BDM17. In the following sections, we report our findings. As mentioned in the abstract, our main finding is the identification of a region in the (σ_{nX}) vs. (m_X) parameter space where constraining DM nucleon scattering cross sections with neutron stars becomes impossible. This is due to the fact that in that region the total capture rate becomes insensitive to both σ_{nX} and m_X . Conversely, for a given ambient dark matter density, we find the maximum temperature a NS of a given mass has to have (T_{crit}) such that it can be used to constrain the neutron dark matter scattering cross section.

II. RESULTS

A. Analytical approximations of the total capture rates

In principle one can calculate, just as in BDM17 and IZ19, the total capture rates by numerically adding the terms in Eq. 1 until the sum has converged, i.e. up to $N_{cut} \sim \tau$. Sometimes this can be computationally expensive, but, more importantly, this procedure obscures the physics. We decided to explore limiting regimes where we were able to analytically approximate the sums. For more details, see [12]. Here we just summarize the results, since we will be using them when comparing our reproductions of Figs. 2-4 of BDM17 with those presented in BDM17.

We start with the definition of the probability that a DM particle will collide exactly N times as it crosses a star, p_N . BDM17 finds $p_N(\tau) = (2/N!) \int_0^1 dy y e^{-y\tau} (y\tau)^N$. In IZ19, we show that this is equivalent to the following closed form:

$$p_N(\tau) = \frac{2}{\tau^2} \left(N + 1 - \frac{\Gamma(N + 2, \tau)}{N!} \right), \quad (4)$$

where $\Gamma(a, b)$ is the incomplete gamma function. From the above form we get the following approximations:

$$p_N(\tau) \approx \begin{cases} \frac{2\tau^N}{N!(N+2)} + \mathcal{O}(\tau^{N+1}), & \text{if } \tau \ll 1 \\ \frac{2}{\tau^2} (N+1) \Theta(\tau - N), & \text{if } \tau \gg 1. \end{cases} \quad (5a)$$

$$\quad (5b)$$

Above $\Theta(\tau - N)$ is the Heaviside step function. Note that after $N \sim \tau$ the actual probability $p_N(\tau)$ from Eq. 4 is rapidly driven to zero because of the Γ term.

In the next section, we will discuss our reproductions of Fig. 2 of BDM17. Namely, we will calculate the mass capture rate $m_X C_X$ as a function of m_X numerically by adding the terms in Eq. 1. Below we are developing semi-analytical closed form approximations for those sums. We start with the general situation, where one cannot use the approximations that lead to the simplified form in of the capture rates C_N presented in Eq. 3. The C_N 's presented in Eq. 2 are quite complicated, but we can make progress by analyzing the limiting behaviour of the exponent:

$$R_v \equiv \frac{3(v_N^2 - v_{esc}^2)}{2\bar{v}^2} \approx \begin{cases} \frac{3}{2}(2^N - 1) \frac{v_{esc}^2}{\bar{v}^2}, & \text{if } m \sim m_X \\ \frac{3}{2} N \frac{m}{m_X} \frac{v_{esc}^2}{\bar{v}^2}, & \text{if } m \ll m_X \end{cases} \quad (6a)$$

$$\quad (6b)$$

Expanding the exponential in Eq. 2 we find:

$$C_N \approx \begin{cases} \frac{1}{3} \left(\frac{6}{\pi} \right)^{1/2} \pi R^2 p_N(\tau) n_X \frac{3v_{esc}^2 + 2\bar{v}^2}{\bar{v}}, & \text{if } R_v \ll 1 \\ \frac{3}{2} \left(\frac{6}{\pi} \right)^{1/2} \pi R^2 p_N(\tau) \frac{n_X v_{esc}^4}{\bar{v}^3} \beta_+ \langle z \rangle (N + N^2 \beta_+ \langle z \rangle), & \text{if } R_v \gg 1. \end{cases} \quad (7a)$$

$$\quad (7b)$$

We point out that the conditions on R_v can be recast as conditions on the ratio between the mass of the target nuclei (m), and the mass of the DM particle (m_X), in view of the definition of v_N in terms of β_+ . This can be explicitly seen from Eqns. 6a and 6b. As a general rule, for masses higher than a limit value that depends on N and the $\frac{v_{esc}^2}{\bar{v}^2}$ ratio the condition $R_v \gg 1$ is met.

What one is ultimately interested in is the total capture rates, or the sum in Eq. 1. We start with semi-analytical results in the appropriate limits for $C_{tot, N_{max}} \equiv \sum_{N=1}^{N_{max}} C_N$, where the sum is cut off at an arbitrary N_{max} . There will be generally two regimes, $\tau \ll 1$ (single scattering), and $\tau \gg 1$. For the latter we get, by using Eqns. 5b, 7a and 7b:

$$C_{tot, N_{max}} \approx \begin{cases} \left(\frac{2}{3\pi}\right)^{1/2} \frac{\pi R^2}{\tau^2} n_X \frac{3v_{esc}^2 + 2\bar{v}^2}{\bar{v}} N_{max}(N_{max} + 3), & \text{if } R_v \ll 1 \text{ (8a)} \\ \left(\frac{6}{\pi}\right)^{1/2} \frac{\pi R^2}{\tau^2} n_X \frac{v_{esc}^4}{\bar{v}^3} \beta_+ \langle z \rangle N_{max}(N_{max} + 1)(N_{max} + 2) \left(1 + \frac{\beta_+ \langle z \rangle}{4} (1 + 3N_{max})\right), & \text{if } R_v \gg 1 \text{ (8b)} \end{cases}$$

We note that the equations above hold only for $N_{max} \leq N_{cut} \sim \tau$. When $N_{max} > N_{cut}$, since the sums are converged, we simply replace N_{max} with τ in the equations above.

In the regime where $m_X \gg m$ and $v_{esc} \gg \bar{v}$ we can calculate C_{tot} analytically, both for multi-scatter ($\tau \gg 1$) and single scatter ($\tau \ll 1$) capture. For details of this calculation see [11]. The main result is that we find a closed form for the following sum:

$$\sum_{N=1}^{\infty} p_N(\tau) \left(1 - \left(1 + \frac{2A_N^2 \bar{v}^2}{3v_{esc}^2}\right) e^{-A_N^2}\right) = T_1 - T_2 - T_3$$

where we define $T_1 \equiv \sum_{N=1}^{\infty} p_N(\tau)$, $T_2 \equiv \sum_{N=1}^{\infty} p_N(\tau) e^{-A_N^2}$, and $T_3 \equiv \sum_{N=1}^{\infty} p_N(\tau) \frac{2A_N^2 \bar{v}^2}{3v_{esc}^2} e^{-A_N^2}$. For the single scatter case the sums are trivial, since this amounts to only keeping the $N = 1$ term in those sums and using the approximate form of $p_N(\tau)$ from Eq. 5a. In fact, for single scattering regime one can immediately get $C_{tot} = C_1$ from Eqns. 7b or 7a. Note that in that case there is a transition between a DM mass independent (Eq. 7b) to a capture rate that is depends on mass via β_+ . For the multiscatter case, we start with the simplest of the three terms, T_1 . In that case, since $\tau \gg 1$, we have: $T_1 = 1 - p_0(\tau) \approx 1$. For $T_2 \equiv \sum_{N=1}^{\infty} p_N(\tau) e^{-A_N^2}$ we find:

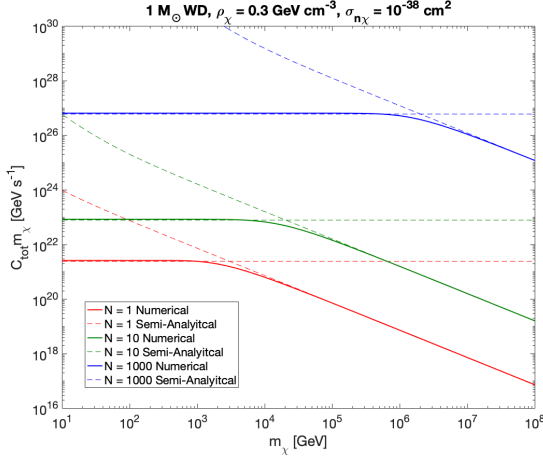
$$\sum_{N=1}^{\infty} p_N(\tau) e^{-A_N^2} = \frac{2e^{-k\tau}(-1 + e^{k\tau} - k\tau)}{(k\tau)^2}, \quad (9)$$

where we introduced a simplifying notation: $k \equiv \frac{3v_{esc}^2}{\bar{v}^2} \frac{m}{m_X}$. For the last term $T_3 \equiv \sum_{N=1}^{\infty} p_N(\tau) \frac{2A_N^2 \bar{v}^2}{3v_{esc}^2} e^{-A_N^2}$ we find:

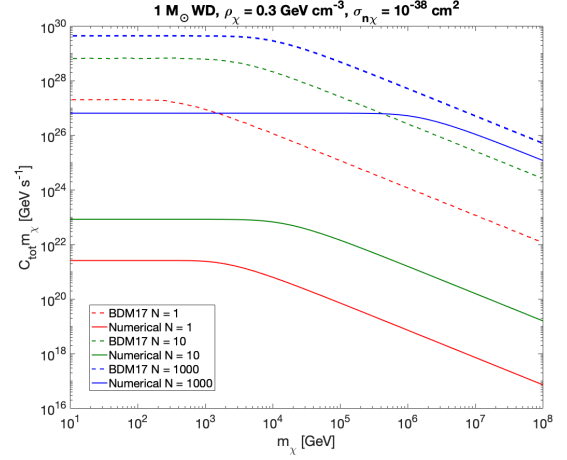
$$\sum_{N=1}^{\infty} p_N(\tau) \frac{2A_N^2 \bar{v}^2}{3v_{esc}^2} e^{-A_N^2} = \frac{4m}{m_X} \frac{e^{-k\tau}(-2 + 2e^{k\tau} - 2k\tau - k^2\tau^2)}{k^3\tau^2}. \quad (10)$$

B. Testing the Analytical approximations

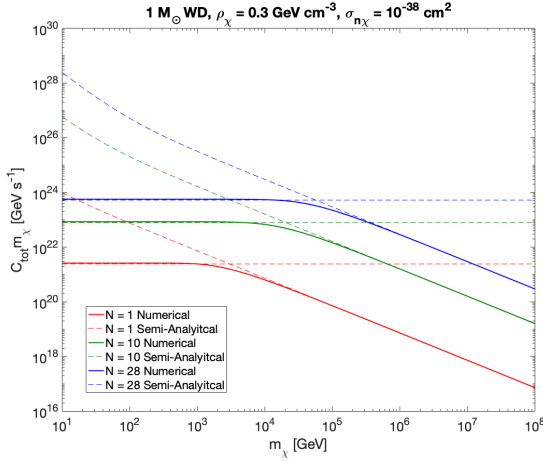
We start by validating our semi-analytical approximations presented in Sec. II A. For this purpose, we calculate the mass capture rates on a constant density white dwarf, similarly to the results of Fig. 2 in BDM17. Here, we find that our semi-analytical results presented in Eqns. 8a and 8b match perfectly with the numerical results obtained by adding term by term C_N 's given by Eq. 2 up to an arbitrary N_{max} . This can be seen in the two left panels of Fig. 1. We point out a severe discrepancy when comparing our results for the mass capture rates when a fixed arbitrary N_{max} is imposed, with those presented in BDM17 for the exact same set of parameters, as one can see from the right side panels of Fig. 1. The fact that our numerical and semi-analytical results match so well leads us to believe that there are some problems in the corresponding results of BDM17. From Eq. 8b we find the expected scaling with N_{max} of the mass capture rate in the regime where it is independent of m_X . Namely, $C_{tot, N_{max}} \sim N_{max}(N_{max} + 3)$. We infer that the quoted value of N_{max} labeled as 1000 in Fig. 2 of BDM17 must be a typo, hence the three values of the mass capture rate for $m_X = 10$ GeV do not obey this scaling. We find that the N_{max} the upper curve must be 28 in order for the three curves to scale as $N_{max}(N_{max} + 3)$. Even after correcting for this, we observe an overall discrepancy of about 6 orders of magnitude between our results and those of BDM17. We cannot speculate as to the reason of behind this discrepancy; however, we mention that we did triple check our numerical results and unit conversion factors. We point out that a similar six orders of magnitude discrepancy was found when we reproduced the right panel of Fig. 2 of BDM17. In the interest of saving space, we omit from including that here, but we are more than happy to make it available to the authors of BDM17.



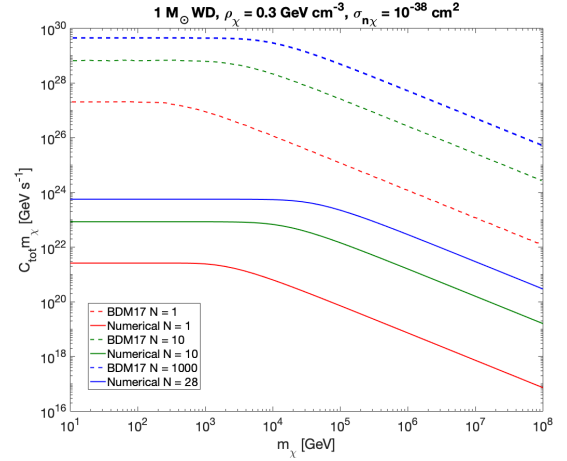
(a) Our full numerical vs. our semi-analytical results



(b) Comparison of our results to BDM17 Fig. 2 left panel



(c) Adjusted N for the third case from 1000 to 28. See discussion below.



(d) Comparison of our results to BDM17 Fig. 2 left panel after adjusting N.

FIG. 1. Mass capture rate of dark matter on a constant density one solar mass white dwarf. For each case value of N_{max} where we arbitrarily truncate the series defining C_{tot} is labeled in the legend. A per-nucleon DM scattering cross section of $\sigma_{n\chi} = 10^{-38} \text{ cm}^2$, an ambient DM density of 0.3 GeV/cm^3 , and $\bar{v} = 220 \text{ km/s}$, and are assumed. Note that form factor effects lead to an effective DM scattering cross section with the target carbon nuclei enhanced by about four orders of magnitude, as explained in BDM17 (See Legend of their Fig. 2).

C. Probing heavy dark matter with old neutron stars

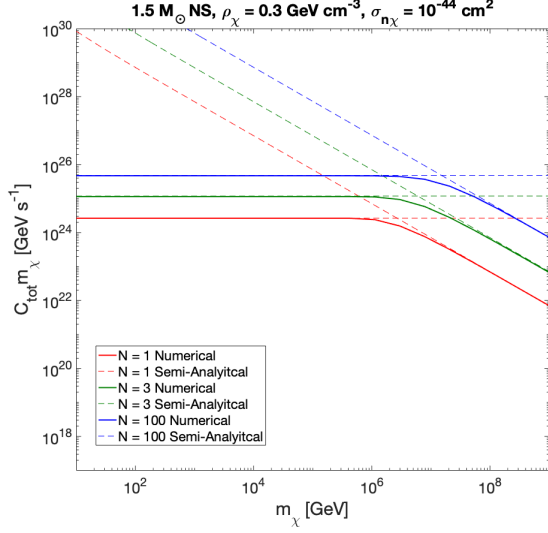
We next move on to replicating the results of Figs. 3 and 4 of BMD17. Namely we are interested in the effects of dark matter capture in neutron stars and follow the implementation of the general relativistic effects in the same way as explained in Sec. III of their paper. The capture rate coefficients C_N are enhanced to:

$$C_N \rightarrow \frac{C_N}{1 - \frac{2GM}{Rc^2}} \quad (11)$$

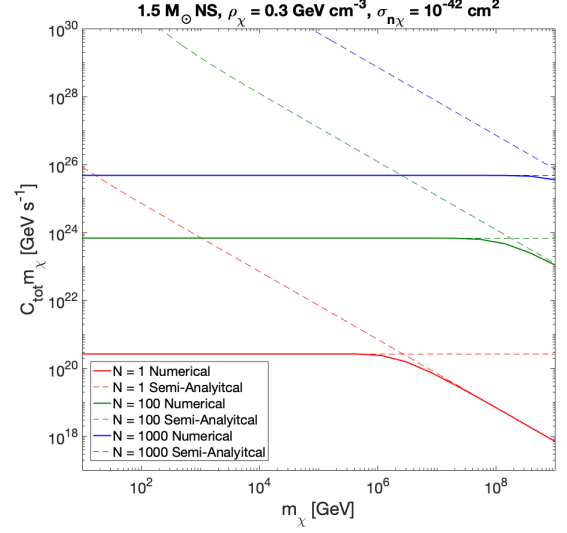
and the escape velocity has to be now calculated in the following way:

$$v_{esc} \rightarrow \sqrt{2\chi}, \quad (12)$$

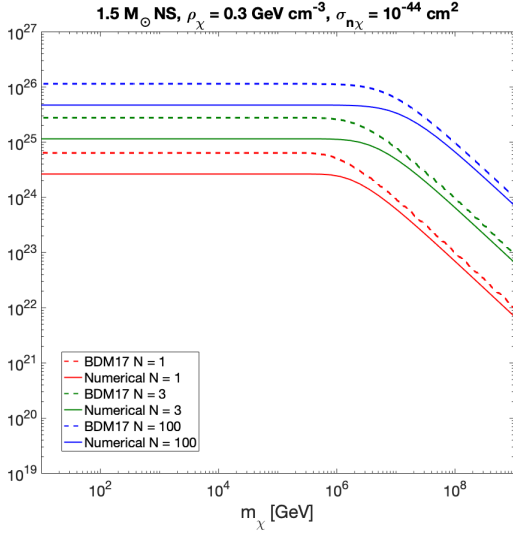
with $\chi = [1 - (1 - 2GM/Rc^2)^{1/2}]$. We first focus, just as we did for the case of WD, on the mass capture rate of dark matter on a neutron star, when adding term by term the C_N s given by Eq. 11 up to an arbitrary cutoff N_{max} . The results are presented in Fig. 2. Just as before, for the case of WDs, we find that the mass capture rates from



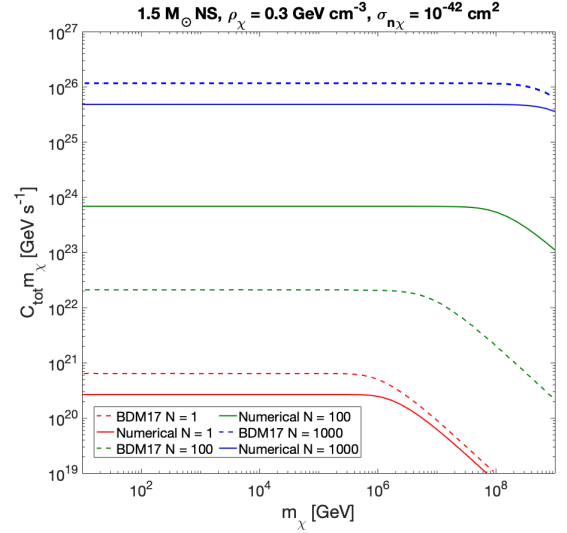
(a) Our full numerical vs. our semi-analytical results for the left panel of Fig. 3 of BDM17



(b) Our full numerical vs. our semi-analytical results for the right panel of Fig. 3 of BDM17



(c) Comparison of our results to BDM17 Fig. 3 left panel



(d) Comparison of our results to BDM17 Fig. 3 right panel

FIG. 2. Mass capture rate of dark matter on a neutron stars. Relevant parameters described above each figure.

BDM17 are above our own estimates. In this case, the discrepancy is much milder however. Just as before, we cannot speculate as to the cause of this discrepancy, but we do confirm that we triple checked our numerical values. Moreover, the agreement we see between our full numerical results and the semi-analytical ones, obtained by using Eqns. 7a and 7b, is very encouraging.

Next, we move to exploring the main topic of BDM17, which is the possibility of using the developed multiscatter formalism to constrain dark matter properties. Fig. 4 of BDM17 shows that upper-bounds on the neutron DM scattering cross section (σ_{nX}) as a function of the dark matter particle mass (m_X) coming from an old NS of a given temperature placed in a DM rich environment, such as the galactic center, can be competitive, at low DM mass regime with direct detection experiments. Most importantly, for DM mass $m_X \gtrsim 10^5$ GeV the neutron stars are more sensitive to DM neutron interactions than current DM direct detection experiments on earth, such as LUX-PandaX [14] or XENON1T [15–17]. And the most exciting finding is that they can be used to probe below the “neutrino floor,” which is a major limitation of any direct detection experiment on Earth.

The basis of the method proposed by BDM17 to use NS as dark matter detectors is briefly explained below. For old NS, an equilibrium between dark matter annihilation and capture can be reached on timescales t_{eq} much less than the

age of the neutron star itself. Moreover, typically, the captured DM thermalizes inside the NS on time scales smaller than t_{eq} . For details, see BDM17 Sec. IV. Therefore, in order to calculate the luminosity generated inside the NS by captured DM annihilations we only need to know the capture rates: $m_X C_X = L_{DM}$. Henceforth, we will denote by $C_X \equiv C_{tot}$, the total capture rate for a given DM particle mass calculated by adding all C_N 's as given by Eq. 11 up to a cutoff, N_{cut} where the series has converged. Assuming the NS is in thermal equilibrium and that at T_{NS} is maintained constant by DM heating:

$$L_{DM} = L_{rad}, \quad (13)$$

where L_{rad} is the rate with which thermal energy is radiated at the surface of the neutron star: $L_{rad} = 4\pi R_{NS}^2 \sigma_0 T_{NS}^4$. If we read it correctly, Eq. 30 of BDM17 seems to just be a restatement of the equation above, with the only change the r.h.s is L_∞ , the apparent observed luminosity of the distant NS, not the thermally radiated power at the surface of the star. For completeness and clarity, below is Eq. 30 of BDM17:

$$m_X C_X = L_{DM} = 4\pi\sigma_0 R^2 T_{NS}^4 (1 - 2GM/Rc^2)^2, \quad (14)$$

where σ_0 is the Stefan-Boltzmann constant. Note that we have introduced a factor of c^2 in the denominator of $2GM/Rc^2$, for clarity and since we did not use natural units throughout any of our numerical calculations. However, unless we are missing something fundamental, we find that there are some problems with the factors of $(1 - 2GM/Rc^2)$ appearing on the r.h.s. of Eq. 30 of BDM17. First, we point out that the heating rate due to DM should be compared to the rate the NS is radiating energy at its surface (L_{rad}), not to the rate observed by an infinitely distant observer (L_∞). This is our statement in Eq. 13. General relativistic effects such as time dilation and gravitational redshift lead to the following relationship between those two quantities [18, 19]:

$$L_\infty = L_{rad}(1 - 2GM/Rc^2), \quad (15)$$

where M and R represent the mass and the radius, respectively, of the compact object, i.e. the NS in our case. Secondly, on the l.h.s. of Eq. 30 of BDM17, one can only assume that L_{DM} is calculated by summing the enhanced mass captured rates $m_X C_N$, with C_N 's rescaled according to Eq. 11. However, in that case the suppression factor on the r.h.s. of Eq. 30 in BDM17 (our Eq. 14) should be $(1 - 2GM/Rc^2)$ (coming from the difference between the apparent luminosity L_∞ and the luminosity at the surface of the neutron star, L_{rad}) not, $(1 - 2GM/Rc^2)^2$, which is the factor in Eq. 14. We did consider that perhaps L_{DM} is actually calculated by not rescaling C_N 's and moving this constant factor to the r.h.s. of Eq. 30 when attempting to reproduce Fig. 4 of BDM17. However, our point is that the bounds on DM parameters coming from the requirement of a NS of a given temperature T_{NS} not overheating should actually be placed from Eq 13, not from Eq. 14, for the reasons explained above. Following this procedure, we get the following equation that will be used to place constraints in the σ_{nX} vs. m_X parameter space:

$$\sum_{N=1}^{\infty} p_N(\tau) \left(1 - \left(1 + \frac{2A_N^2 \bar{v}^2}{3v_{esc}^2} \right) e^{-A_N^2} \right) = 4.6 \frac{R_{NS}}{R_{10}} \frac{\bar{v}}{v_{220}} \frac{M_{1.5}}{M_{NS}} \left(1 - \frac{r_S}{R_{NS}} \right)^p \frac{(T_{NS}/T_{30,000})^4}{\rho_X/\rho_{1000}}, \quad (16)$$

where we introduced the following simplifying notations: $R_{10} \equiv 10$ km, $v_{220} \equiv 220$ km/s, $M_{1.5} \equiv 1.5 M_\odot$, $r_S \equiv 2GM_{NS}/R_{NS}c^2$, $T_{30,000} \equiv 3 \times 10^4$ K, and $\rho_{1000} = 10^3$ GeV cm $^{-3}$. Also note that we have replaced the sign of the parenthetical term in the left hand side to + form -, for reasons explained before (see discussion above Eq. 3). We leave the term general relativistic corrections term as $\left(1 - \frac{r_S}{R_{NS}} \right)^p$. BDM17 has $p = 2$, however, as explained above, we believe the right value to use is $p = 1$. There are several things we note about Eq. 16. First, the left hand side is *always* less or equal to unity. This is obviously the case, since:

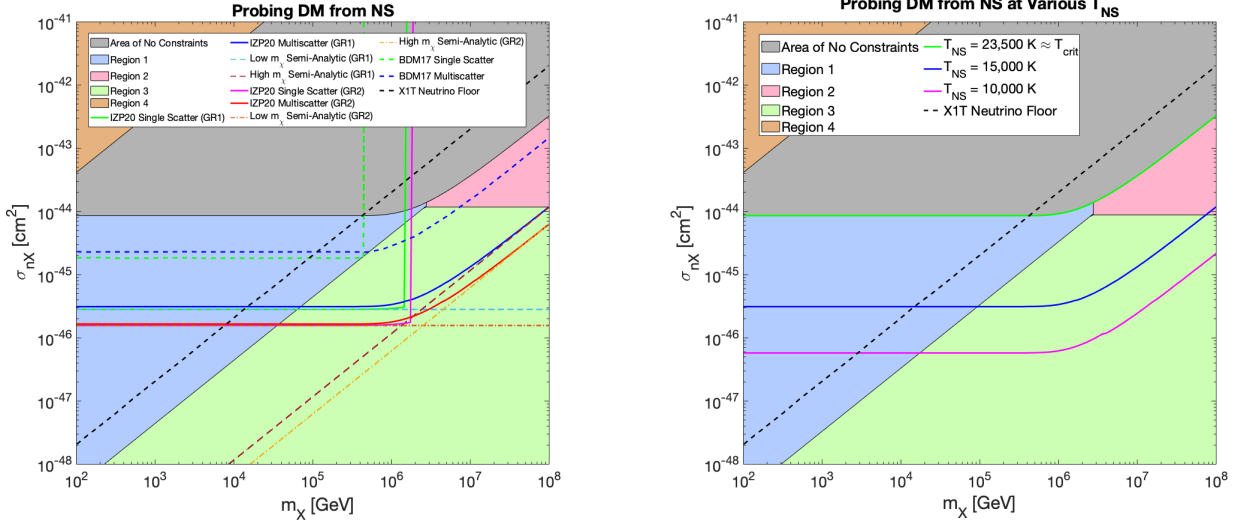
$$\sum_{N=1}^{\infty} p_N(\tau) \left(1 - \left(1 + \frac{2A_N^2 \bar{v}^2}{3v_{esc}^2} \right) e^{-A_N^2} \right) \leq \sum_{N=1}^{\infty} p_N(\tau) \leq \sum_{N=0}^{\infty} p_N(\tau) = 1.$$

This realization places a limit on the temperature of the NS, at a given dark matter density and halo dispersion velocity, for which the old neutron stars can be used as DM detectors. For NS with surface temperatures larger than this critical temperature, $T_{NS} \gtrsim T_{crit}$, one cannot use the NS as probes of dark matter, since the R.H.S. of Eq. 16 becomes larger than 1. For T_{crit} we get:

$$T_{crit} = 2.04 \times 10^4 \text{ K} \left(1 - \frac{r_S}{R_{NS}} \right)^{-p/4} \left(\frac{R_{10}}{R_{NS}} \frac{M_{NS}}{M_{1.5}} \frac{v_{220}}{\bar{v}} \frac{\rho_X}{\rho_{1000}} \right). \quad (17)$$

We note that for the parameters used in BDM17 and with $p = 2$, as appropriate for their calculation, we get $T_{crit} \approx 27,400$ K. Using $p = 1$ changes this value to even lower, $T_{crit} \approx 24,000$ K. The key point is that both of

those values are smaller than 30,000 K, the value quoted in BDM17 for their exclusion limit presented in their Fig. 4. This is very puzzling since, as we demonstrated above, for $T_{NS} > T_{crit}$ one cannot use NS to place constraints on DM properties. Again, we cannot speculate as to how BDM17 manages to place those constraints presented in their Fig. 4 for a NS of $T_{NS} \sim 3 \times 10^4$ K, as mentioned in the legend of their Fig. 4. However, we do mention that, as expected, running our codes for $T_{NS} = 30,000$ K fails to produce a solution. In Fig. 3a We present the bounds we get for a NS with temperature $T_{NS} = 1.5 \times 10^4$ K and contrast those with the ones from Fig. 4 of BDM17. In Fig. 3b we show the bounds on the neutron DM scattering cross section implied by the observation at the galactic center of NS of temperatures ranging from T_{crit} all the way down to $T_{NS} = 10,000$ K. We discuss below our main conclusions and



(a) Our (IZP20) full numerical (solid blue and red lines) and our semi-analytical results (dashed light blue and maroon, and dotted dashed orange and brown lines) vs. BDM17 (dashed green and blue lines). Note that we consider both cases of $p = 1$ (GR1) and $p = 2$ (GR2). As pointed out in the text $p = 1$ is the correct value, but we believe BDM17 had $p = 2$

(b) Bounds on neutron dark matter scattering cross section σ_{nX} from the potential observation of a 15000 K neutron star in the galactic center region (blue line) and a 10000 K neutron star (purple line). Note that this is a cleaned up version of the figure on the left panel.

FIG. 3. Constraints in neutron DM scattering cross section (σ_{nX}) and dark matter mass (m_X) parameter space coming from the potential observation of a $1.5M_\odot$ neutron star of various temperatures in the galactic center region. For the DM halo parameters we assume $\bar{v} = 220$ km/h and a dark matter density at the center of the halo $\rho_X = 10^3$ GeVcm $^{-3}$. For discussion about the various shaded regions labeled 1-4 and how we obtained our semi-analytical approximation see discussion in the main body of the article.

results extracted from Fig. 3. We start with the shaded regions. The most interesting one, shaded in gray, corresponds to a region in the DM parameter space where old NS at the galactic center cannot be used as detectors. This region is defined as the constraints obtained by assuming a NS with $T_{NS} \approx T_{crit}$. For higher temperatures the r.h.s. of the equation that is used to place those constraints (Eq. 16) becomes larger than unity, whereas the l.h.s. is, by definition less than one. Next we move to the regions labeled 1-4. Region 1 (blue) corresponds roughly to $k\tau \gg 1$ and $\tau \ll 1$. In this region, the single scatter approximation holds, and therefore the l.h.s. of Eq. 16 can be approximated with the first term, for which $N = 1$. Moreover, since $k\tau \gg 1$, we can ignore the exponentially suppressed term, so the entire l.h.s. becomes $p_1(\tau) \approx 2\tau/3$. Since $\tau \propto \sigma_{nX}$ and is independent of m_X , the constraints in this region correspond to constant values of σ_{nX} , as we can see from both our full numerical results and the semi-analytical approximations. Region 2 (pink) corresponds to $\tau \gg 1$ and $k\tau \gg 1$. In this region we can use the analytical approximations of Eq. 9 and Eq. 10 to show that the l.h.s. of Eq. 16 is approximately equal to $2k\tau/3 \propto \sigma_{nX}/m_X$. For this reason the constraints approach, as we transition to region 2, to $\sigma_{nX} \propto m_X$. The green region (3) captures the transition between the two regimes described above. The brown shaded region (4) corresponds to the area where the term in Eq.23 of BDM17 that has the wrong sign (see discussion below our Eq. 3) would become important. In all other regions, that term is sub dominant, and thus irrelevant. In the next section we summarize our results.

III. SUMMARY AND CONCLUSION

For clarity, we briefly summarize our results below. In Sec. I, we point out several errors and typos in BDM17, the paper that has extended the DM capture formalism to the multiscattering regime. First, we identify a missing factor of $1/3$ in the equation giving the capture rate coefficient C_N (Eq. 22 in BDM17 vs. Eq. 2 in this paper). Secondly, we point out a wrong sign in the approximation of the capture rates coefficients C_N when the escape velocity is much greater than the DM halo dispersion velocity, and the mass of the DM particle is much larger than the mass of the target nuclei (Eq. 23 of BDM17 vs. Eq. 3 of this paper). In Sec. II A, we develop semi-analytical approximation for the mass capture rates in various regimes (Eqns. 6b, 6a, 9, and 10). We proceeded to validate those semi-analytical approximation in Sec. II B and Sec. II C. In the process, we identify some errors in Figs. 2, 3, and 4 of BDM17. We would be happy to share with the authors of BDM17 the details of our calculations, such as our Matlab and Mathematica codes.

Our results related to the possibility of using neutron stars as dark matter detectors are presented in Sec. II C. BDM17 requires that a NS does not overheat by, apparently, comparing the intrinsic luminosity due to DM self annihilations to the observed luminosity by a distant observer. We point out that this is conceptually inadequate, as we believe the bounds on DM scattering cross sections should be obtained from requiring that the intrinsic luminosity due to captured DM annihilations does not exceed the rate with which the energy is radiated at the surface of the neutron star. Independent of this subtlety, our most important finding is the identification of a critical temperature (see Eq. 17) above which a NS cannot act as a DM detector.

In summary, we believe that we have pointed out several problems with BDM17 and that we have successfully corrected them. In addition, we developed and validated several important semi-analytical approximations for capture rates of DM in the multiscattering regime, that could be very useful for future research, as full numerical calculations can become computationally expensive. The main conclusion is that old NS at the galactic center remain promising candidates for constraining properties of dark matter below the neutrino floor, as first pointed out in BDM17. However, we disagree with the values presented in BDM17 for the bounds imposed on the dark matter neutron scattering cross section by a potential detection of an old NS of any given temperature near the galactic center.

-
- [1] W. H. Press and D. N. Spergel, *Astrophys. J.* **296**, 679 (1985), [277(1985)].
 - [2] A. Gould, *ApJ* **321**, 571 (1987).
 - [3] K. Freese, D. Spolyar, and A. Aguirre, *JCAP* **0811**, 014 (2008), arXiv:0802.1724 [astro-ph].
 - [4] F. Iocco, *Astrophys. J.* **677**, L1 (2008), arXiv:0802.0941 [astro-ph].
 - [5] C. Kouvaris and P. Tinyakov, *Phys. Rev. D* **82**, 063531 (2010), arXiv:1004.0586 [astro-ph.GA].
 - [6] I. V. Moskalenko and L. L. Wai, in *The First GLAST Symposium*, American Institute of Physics Conference Series, Vol. 921, edited by S. Ritz, P. Michelson, and C. A. Meegan (2007) pp. 508–509, arXiv:0704.1324 [astro-ph].
 - [7] J.-S. Niu, W. Zong, and H.-F. Xue, arXiv e-prints, arXiv:1703.10104 (2017), arXiv:1703.10104 [astro-ph.HE].
 - [8] I. F. M. Albuquerque, L. Hui, and E. W. Kolb, *Phys. Rev. D* **64**, 083504 (2001), arXiv:hep-ph/0009017 [hep-ph].
 - [9] J. Bramante, A. Delgado, and A. Martin, *Phys. Rev. D* **96**, 063002 (2017), arXiv:1703.04043 [hep-ph].
 - [10] B. Dasgupta, A. Gupta, and A. Ray, *JCAP* **08**, 018 (2019), arXiv:1906.04204 [hep-ph].
 - [11] C. Ilie and S. Zhang, *JCAP* **12**, 051 (2019), arXiv:1908.02700 [astro-ph.CO].
 - [12] C. Ilie, J. Pilawa, and S. Zhang, (inpreparation, unpublished) (2020).
 - [13] C. Ilie and S. Zhang, *JCAP* (2020).
 - [14] A. Tan, M. Xiao, X. Cui, X. Chen, Y. Chen, D. Fang, C. Fu, K. Giboni, F. Giuliani, H. Gong, and et al., *Physical Review Letters* **117** (2016), 10.1103/physrevlett.117.121303.
 - [15] E. Aprile, M. Alfonsi, K. Arisaka, F. Arneodo, C. Balan, L. Baudis, B. Bauermeister, A. Behrens, P. Beltrame, K. Bokeloh, and et al., *Physical Review Letters* **109** (2012), 10.1103/physrevlett.109.181301.
 - [16] E. Aprile and et al. (XENON Collaboration 7), *Phys. Rev. Lett.* **121**, 111302 (2018).
 - [17] E. Aprile and et al. (XENON Collaboration 4), *Phys. Rev. Lett.* **122**, 141301 (2019).
 - [18] K. S. Thorne, *ApJ* **212**, 825 (1977).
 - [19] P. Haensel, *A&A* **380**, 186 (2001), arXiv:astro-ph/0105485 [astro-ph].